Published in final edited form as:

Mol Cancer Ther. 2014 August ; 13(8): 1979–1990. doi:10.1158/1535-7163.MCT-13-0963.

Selective Activity of the Histone Deacetylase Inhibitor AR-42 against Leukemia Stem Cells: A Novel Potential Strategy in Acute Myelogenous Leukemia

Monica L. Guzman[1], **Neng Yang**[1], **Krishan K. Sharma**[1], **Marlene Balys**[3], **Cheryl A. Corbett**[3], **Craig T. Jordan**[6], **Michael W. Becker**[3], **Ulrich Steidl**[4], **Omar Abdel-Wahab**[5], **Ross L. Levine**[5], **Guido Marcucci**[7], **Gail J. Roboz**[1], and **Duane C. Hassane**[2]

[1]Division of Hematology/Medical Oncology, Department of Medicine, Weil Medical College of Cornell University, New York

[2]Institute of Computational Biomedicine, Weil Medical College of Cornell University, New York

[3]James P. Wilmot Cancer Center, University of Rochester School of Medicine, Rochester

[4]Department of Cell Biology, Albert Einstein College of Medicine, Bronx

[5]Human Oncology and Pathogenesis Program and Leukemia Service, Memorial Sloan-Kettering Cancer Center, New York, New York

[6]Department of Medicine, University of Colorado Denver, Aurora, Colorado

[7]Division of Hematology, The Comprehensive Cancer Center, College of Pharmacy, Ohio State University, Columbus, Ohio

Abstract

Most patients with acute myelogenous leukemia (AML) relapse and die of their disease. Increasing evidence indicates that AML relapse is driven by the inability to eradicate leukemia

Corresponding Authors: Monica L. Guzman, Weill Medical College of Cornell University, 1300 York Avenue, Box 113, New York, NY 10065. Phone: 212-746-6838; Fax: 212-746-8866; mlg2007@med.cornell.edu; and Duane C. Hassane, Weill Medical College of Cornell University, 1305 York Avenue, Box 140, New York, NY 10021; Phone: 646-543-8263; dhassane@med.cornell.edu.
M.L Guzman and N. Yang contributed equally to this article.

Disclosure of Potential Conflicts of Interest: D.C. Hassane has received honorarium from ARNO Therapeutics. No potential conflicts of interest were disclosed by the other authors.

Supplementary Material: Access the most recent supplemental material at: http://mct.aacrjournals.org/content/suppl/2014/06/16/1535-7163.MCT-13-0963.DC1.html

Authors' Contributions: **Conception and design:** M.L. Guzman, C.T. Jordan, G.J. Roboz, D.C., Hassane
Development of methodology: M.L. Guzman, D.C. Hassane
Acquisition of data (provided animals, acquired and managed patients, provided facilities, etc.): M.L. Guzman, K.K. Sharma, C.A. Corbett, R.L., Levine, G. Marcucci, G.J. Roboz
Analysis and interpretation of data (e.g., statistical analysis, biostatistics, computational analysis): M.L. Guzman, N. Yang, K.K. Sharma, U. Steidl, O. Abdel-Wahab, G. Marcucci, D.C. Hassane
Writing, review, and/or revision of the manuscript: M.L. Guzman, N. Yang, K.K. Sharma, C.T. Jordan, M.W. Becker, U. Steidl, G. Marcucci, D.C. Hassane
Administrative, technical, or material support (i.e., reporting or organizing data, constructing databases): M.L. Guzman, N. Yang, M. Balys, M.W. Becker, D.C. Hassane
Study supervision: M.L. Guzman, N. Yang, D.C. Hassane

stem cells (LSC). Thus, it is imperative to identify novel therapies that can ablate LSCs. Using an *in silico* gene expression-based screen for compounds evoking transcriptional effects similar to the previously described anti-LSC agent parthenolide, we identified AR-42 (OSU-HDAC42), a novel histone deacetylase inhibitor that is structurally similar to phenylbutyrate, but with improved activity at submicromolar concentrations. Here, we report that AR-42 induces NF-κB inhibition, disrupts the ability of Hsp90 to stabilize its oncogenic clients, and causes potent and specific cell death of LSCs but not normal hematopoietic stem and progenitor cells. Unlike parthenolide, the caspasedependent apoptosis caused by AR-42 occurs without activation of Nrf-2-driven cytoprotective pathways. As AR-42 is already being tested in early clinical trials, we expect that our results can be extended to the clinic.

Introduction

Acute myelogenous leukemia (AML) blasts comprise a heterogenous population of malignant cells, a minor subset of which have the ability to give rise to leukemia in immunodeficient mice (1, 2). This rare population of cells is known as leukemia stem cells (LSC) or leukemia-initiating cells. In patients with AML, the frequency of LSCs strongly correlates with adverse clinical outcome (3–5). Indeed, gene expression signatures for LSCs, defined by phenotype or ability to engraft in immunodeficient mice, have been correlated with poor prognosis (6, 7).

LSCs are usually found in a quiescent state, which confers resistance to conventional AML chemotherapeutics, most of which are cell cycle specific (8, 9). Thus, even those patients who achieve complete remission are destined to relapse and succumb to their disease. This fundamental treatment failure suggests that the LSC compartment is not effectively eradicated by the currently available treatments and that novel compounds targeting LSCs specifically are essential to improve clinical outcomes in patients with AML.

We have previously reported that the transcription factor NF-κB represents a therapeutic target in AML as it is constitutively activated in bulk, progenitor, and LSCs but not in normal hematopoietic stem cells (HSC; refs. 10). To date, different strategies that involve NF-κB inhibition have been shown to selectively induce cell death in LSCs without harming their normal counterparts (9–13). Among them is the plant-derived compound parthenolide (12), for which antileukemic activity for blast, stem, and progenitor cells has been demonstrated. However, parthenolide has poor solubility and bioavailability, which limits its clinical utility (14). Parthenolide analogues with improved pharmacologic properties are under development (9).

Considering parthenolide as a prototype of drugs that are active against LSCs, we recently sought to identify novel compounds with parthenolide-like properties using an *in silico* screen of the publicly available gene expression microarray data using the gene expression signature of parthenolide as a probe (13). Importantly, *in silico* approaches also revealed that treatment of LSCs with parthenolide elicited cytoprotective responses driven by activation of the PI3K/mTOR pathway and Nrf2 transcription targets. These, in turn, caused Nrf2-mediated activation of antioxidant response genes, such as *HMOX1*, that could ultimately lead to decreased antileukemic efficacy. Indeed, pharmacologic inhibition of the Nrf2

cytoprotective response with mTOR/PI3K inhibitors improved therapeutic response of parthenolide in mice (15, 16). Here, we demonstrate the potent anti-LSC activity of AR-42 (OSU-HDAC42) as suggested by further gene expression–based *in silico* screens (17, 18).

AR-42 has been reported to be a member of a novel class of HDAC inhibitors structurally similar to phenylbutyrate, but with improved pharmacologic activity in the submicromolar concentrations (18–20). This compound is 26% orally bioavailable (21) and demonstrates significant antitumor properties (17). Early clinical trials with AR-42 are ongoing in both solid tumors and hematologic malignancies.

Consistent with the similarities to parthenolide suggested by *in silico* data, we found that AR-42 demonstrates the ability to potently suppress NF-κB activation in bulk, stem, and progenitor AML. AR-42–mediated apoptosis results in the activation of caspase-8 and PARP cleavage. Notably, in contrast to parthenolide, AR-42 does not activate Nrf2-controlled cytoprotective responses. Finally, we found that AR-42 can induce inhibition of Hsp90, as determined by the degradation of client proteins such as FLT-3. These findings provide a strong scientific rationale for further exploration of AR-42 as a potential LSC-targeted therapeutic agent.

Materials and Methods

Cell isolation and culture

Primary human AML cells (Table 1) were obtained from volunteer donors with informed consent under Weill Medical College of Cornell University (WCMC; New York, NY) Institutional review board approval. Mononuclear cells were isolated from the samples using Ficoll-Paque (Pharmacia Biotech) density gradient separation. Cells were cryopreserved in CryoStor CS-10 (Stem Cell Technologies). Cells were cultured in serum-free medium (22) supplemented with cytokines (50 ng/mL rhFLT-3 ligand, 50 ng/mL rhSCF, 20 ng/mL rhIL3, 20 ng/mL rhIL6) for 1 hour before the addition of drugs. HL-60 (purchased 9/2010, ATCC), KG-1 (purchased 9/2010; ATCC), TF-1 (purchased 9/2010; ATCC), THP-1 (purchased 9/2010; ATCC), Kasumi-1 (purchased 4/2011; ATCC), TUR (purchased 1/2010; ATCC), U937 (purchased 12/2009; ATCC), and MOLM-13 [a kind gift from G. Chiosis (Memorial Sloan-Kettering Cancer Center, MSKCC); 7/2010, 2/2014 authenticated; Biosynthesis]. Cell lines were cultured in Iscove's modified Dulbecco's medium (Life Technologies) supplemented with 10% to 20% FBS according to culture conditions indicated by the ATCC and 1% penicillin/streptomycin (Pen/Strep; Life Technologies). Parthenolide was obtained from Biomol and AR-42 was provided by ARNO Therapeutics.

Flow cytometry

Apoptosis assays were performed as described previously (10). Briefly, after 24 to 48 hours of treatment, primary cells were stained for the surface antibodies CD34-allophycocyanin (APC), CD38-phycoerythrin with cyanin-7 (PECy7), CD123-phycoerythin (PE), and CD45-allophycocyanin-Hilite.7-BD (APC-H7; Becton Dickinson,) for 15 minutes. Cells were washed in cold PBS and resuspended in 200 μL of Annexin-V buffer (0.01mol/L HEPES/NaOH, 0.14 mol/L NaCl, 2.5 mmol/L $CaCl_2$) containing Annexin-V-FITC or Annexin-V-

PE (Becton Dickinson) and 7-aminoactinomycin (7-AAD, Life Technologies). Cells were incubated at room temperature for 15 minutes then analyzed on a BDLSRII flow cytometer using the high throughput attachment. To analyze human cell engraftment in the NOD/SCID xenotransplant model, bone marrow cells were blocked with the anti-Fc receptor antibody 2.4G2 and 25% human serum and later labeled with anti-human CD45-PE and anti-mouse CD45-FITC antibodies (Becton Dickinson). For reactive oxygen species (ROS) detection, the cells after treatment were incubated with 5 mmol/L CellROX Green Reagent (Life Technologies). The staining for CD117 was performed on MV4–11 cells after treatment with AR-42 or HSP90i using anti-human CD117-PE antibody (Becton Dickinson). Specific active caspase-3 antibody was used according to the manufacturer's protocols (BD Pharmingen).

Microarray gene expression profiling

AML cell lines (MOLM-13 and THP-1 cells) and $CD34^+$ AML cells from two patients were exposed to 0.25 μmol/L AR-42 for 6 hours alongside vehicle-treated controls. AR-42 gene expression profiles were captured using Illumina BeadChip HT12v4 chips (Illumina, Inc.) and analyzed using R/BioConductor (23). Gene expression values were determined and quantile normalization was performed using the beadarray package (24). Parthenolide gene expression profiles are deposited in Gene Expression Omnibus (GEO) accession number GSE7538.

Comparison of AR-42 and parthenolide gene expression profiles

Similarity of the AR-42 gene expression profile to the parthenolide gene expression profile was determined using GSEA software obtained from the Broad Institute (Cambridge, MA; ref. 25). Gene perturbations resulting from AR-42 exposure of AML cells were compared against the 150 gene signatures reported previously (13), collapsing both Illumina and Affymetrix identifiers to gene symbols to facilitate this comparison. Gene sets consisting of genes either upregulated or downregulated by parthenolide were compared with the AR-42 signature using GSEAPreranked analysis with 1,000 permutations.

Pathway and network analysis

Following quantile normalization, differentially expressed genes were determined using Limma followed by Benjamini–Hochberg adjustment of *P* values to control the false discovery rate (26, 27). Overrepresented pathways among differentially expressed genes were determined using DAVID pathway analysis (28) and the BioConductor packages, ReactomePA (29) and cluster-Profiler (30). ClusterProfiler networks were exported to GraphML format, using igraph (31) and visualized using CytoScape 2.8.1 with the GraphMLReader plugin (32).

Methylcellulose colony-forming assay

Primary AML cells were cultured as above for 24 hours in the presence or absence of AR-42. Cells were plated at 50,000 cells/mL in Methocult GFH4534 (Stem Cell Technologies) supplemented with 3 U/mL erythropoietin and 50 ng/mL G-CSF. Colonies were scored after 10 to 14 days of culture.

NOD/SCID mouse assays

NOD/SCID mice were sublethally irradiated with 270 rad using a RadSource-2000 X-ray irradiator before transplantation. Cells to be assayed were injected via tail vein (5-10 million cells) in a final volume of 0.2 mL of PBS with 0.5% FBS. After 6 to 8 weeks, the animals were sacrificed, and bone marrow was analyzed for the presence of human cells by flow cytometry. All animal studies were performed under WCMC Institutional Animal Care and Use Committee approved protocol.

Immunoblots

Cells were prepared and analyzed as previously described (15). Blots were probed with antibodies specific for either heme oxygenase 1 (Millipore), cleaved caspase-8, cleaved PARP, phospho-NF-κBp65 (Ser536), phospho-p70-S6-Kinase (Thr389), phospho-p44/42 MAPK (Erk1/2; Thr202/Tyr204; Cell Signaling Technology), HSP90α/β (F-8), FLT-3/FLT-2 (Santa Cruz Biotechnology), or β-actin (Sigma).

Immunoprecipitation of histone H3

Cell lysates were incubated with Histone H3 antibody for 1 hour at 4°C. Washed protein A/G-agarose beads were added to the cell lysate and antibody mixture and incubated overnight at 4°C. Immunoprecipitates were washed three times, and proteins were eluted with SDS sample loading buffer. The immunoblotting was performed with antibodies against histone-H3 (Santa Cruz Biotechnology), and acetylated lysine (Cell Signaling Technology).

Quantitative reverse transcription PCR

Total RNA was extracted from cultured cell lines or isolated $CD34^+/CD38^-$, $CD34^+/CD38^+$, and $CD34^-$ populations. RNA extraction was performed using the RNeasy Mini Kit (Qiagen) according to the manufacturer's instructions. Quantitative reverse-transcription PCR (qPCR) was assessed by TaqMan RNA-to Ct 1-Step Kit using the StepOnePlus Real-Time PCR System (Applied Biosystems). HMOX1 was assayed using probe Hs01110250_m1, GCLM using Hs00157694_m1, NQO1 using Hs02512143_s1, NFKB1 using Hs00765730_m1, HSP70 using Hs00359163_s1, GAPDH using Hs02758991_g1, BCL2 using Hs00608023_m1, MYB using Hs00920556_m1, TNFSF13B using Hs00198106_m1, PLAU using Hs01547054_m1, CDK6 using Hs01026371_m1, ECH1 using Hs01061992_g1, BCL11A using Hs01093197_m1, TGIF2 using Hs00904994_g1, LMO2 using Hs00153473_m1, KIT using Hs00174029_m1, STIP1 using hs00428979_m1, SQSTM1 using hs00177654_m1, HSPA1B using Hs01040501_sH, MAP1LC3 using hs01076567_g1. All probes were obtained from Applied Biosystems (Life Technologies).

Measurement of NF-κb p65 and Nrf2 activities

NF-κB- and Nrf2-binding activity assays were performed according to the manufacturer's instructions (TransAM NF-κB p65 Chemi or TransAM Nrf2; Active Motif) using nuclear extracts prepared from cells either untreated or treated for 6 hours with 7.5 μmol/L parthenolide or 1 μmol/L AR-42.

Analysis of intracellular thiol levels

Cellular thiol levels were evaluated with mBBr (Life Techologies). mBBr was prepared as a 5 mmol/L solution in 100% ethanol and stored at −20°C. After treatment, cells were labeled with 50 μmol/L mBBr for 15 minutes at 37°C in PBS. After labeling, cells were washed with PBS and resuspended in FACS buffer (0.5% FBS in PBS) containing 1 μg/mL of 7-AAD (Life Technologies).

Statistical analysis

Statistical analyses and graphs were performed using GraphPad Prism software (GraphPad Software). For statistical analysis, the data were log transformed and analyzed by one-way ANOVA followed by the Tukey *post hoc* test. For two-group comparisons, significance was determined by paired *t* tests.

Results

Gene expression-based *in silico* screen reveals similarity between parthenolide and AR-42

We previously reported the ability to use the transcriptional perturbations arising from parthenolide exposure of $CD34^+$ AML as a means of identifying potential parthenolide-like compounds using data in the GEO (13). AR-42 (GSM197171) was identified as a parthenolide-like compound among the top hits upon subsequently querying 23,129 records in the GEO. This public gene expression profile captured gene expression changes modulated by AR-42 following a 6-hour challenge with acid-induced stress in the human SEG-1 esophageal adenocarcinoma cell line (33). To investigate the similarity of transcriptional changes evoked by AR-42 to that of transcriptional changes evoked by parthenolide in AML, we exposed $CD34^+$ primary AML cells and AML cell lines (MOLM-13 and THP-1 cells) to 0.25 μmol/L AR-42 for 6 hours alongside vehicle-treated controls, and captured transcriptional profiles on the Illumina HumanHT12v4 BeadChips. This profiling approach revealed profound pre- versus posttreatment transcriptional changes affecting 988 genes. Thus, we compared the similarity of the AR-42-induced transcriptional changes to the parthenolide gene signature used to interrogate GEO (33). As expected, gene-set enrichment analysis (GSEA; ref. 25) demonstrated significant similarities between the patterns of gene expression changes evoked by AR-42 and parthenolide for both upregulated ($P < 0.01$) and downregulated ($P < 0.05$) genes (Fig. 1A). To confirm that AR-42 demonstrates an HDAC inhibitor activity, we performed GSEA and biochemical analysis indicating the expected similarity to other HDAC inhibitors such as SAHA and trichostatin A at the transcriptional level (GSEA) and the functional level (immunoprecipitation studies of histone H3 demonstrating increased acetylated lysine with AR-42 treatment; Supplementary Fig. S1A and S1B). Leading-edge analysis of the GSEA results identified a subset of 22 downregulated and 19 upregulated genes common between AR-42 and parthenolide, including genes encoding Hsp70 (*HSPA1A* and *HSPA1B*) and c-Kit (*KIT*; Fig. 1B). A qPCR analysis of 10 of these genes confirmed the same pattern of up- and downregulation, validating the similarity (Supplementary Fig. S1C). Pathway analysis of the AR-42 gene signature indicated the ability of AR-42 to perturb pathways relating to NF-κB, as previously noted for parthenolide (ref. 12; Supplementary Tables S1–S4; for gene list see Supplementary Table S5). Taken together, the *in silico* screen identified AR-42 as a

parthenolide-like antileukemic agent with a common gene expression signature that indicated NF-κB inhibitory activity. Given the similarities suggested by gene signature analysis, we proceeded to compare the functional similarities between parthenolide and AR-42 and assessed its anti-AML efficacy.

AR-42 is a potent antileukemic agent

To determine the ability of AR-42 to kill leukemia cells, we first tested AR-42 in a panel of 9 phenotypically and molecularly distinct AML cell lines, including KG-1, Kasumi-1, HL-60, MOLM-13, MV4–11, U937, TUR, THP-1 and TF-1. AR-42 induced cell death in all cell lines tested, with a mean LD_{50} of 0.478 μmol/L (n = 8). THP-1 cells did not effectively respond to treatment with increasing concentrations up to 5 μmol/L of AR-42 (Supplementary Fig. S2, top; Table 2). In contrast, the activity of parthenolide was not as robust against the same panel of cell lines at similar concentrations (average LD_{50} >10 μmol/L; $P < 0.001$; Kolmogorov–Smirnov test; Supplementary Fig. S2, bottom). In addition, AR-42 activity was also assessed in 15 primary AML samples (Table 1) and compared with commonly used chemotherapy drugs, such as cytarabine. The samples included specimens with known *DNMT3A*, *TET2*, and *FLT3* mutational status (Fig. 2). We found that the response of primary blasts to cytarabine was variable. For example, blasts with poor prognosis DNMT3A and TET2 mutations were more resistant to cytarabine (Fig. 2 middle; for e.g., AML2, AML7; refs. 6, 34). Cytarabine treatment produced a median viability of 55% across these samples at a concentration of 5 μmol/L, with minimal change at 10 μmol/L concentration (44%) at 48 hours. Furthermore, parthenolide treatment resulted in a median viability of 26% at a concentration of 10 μmol/L. Interestingly, 3 of 4 TET2 mutant primary AML samples tested were also relatively resistant to parthenolide (Fig. 2, bottom). In contrast, AR-42 induced cell death in 14 of 15 primary AML samples tested, independent of their genotype, at a mean LD_{50} of 0.810 μmol/L (Fig. 2, top; Table 2). The single primary AML sample (AML8) with an incomplete response to AR-42 (40% cell death at 5 μmol/L AR-42) was also resistant to parthenolide. The median viability for the primary AML samples was 25% at 1.25 μmol/L of AR-42. Together, these data indicate that AR-42 has a potent antileukemic activity, as suggested by the transcriptionbased screen.

AR-42 demonstrates activity against leukemia stem cells

Since the *in silico* screen suggested AR-42 as a parthenolide-like compound, we also investigated the ability of AR-42 to ablate leukemia stem and progenitor cells as described for parthenolide (12). Indeed, treatment with AR-42 resulted in decreased viability of phenotypically defined LSCs ($CD34^+CD38^-$ $CD123^+$; Fig. 3A and B, left). In contrast, as previously reported by us and others (11, 35), LSCs were not effectively killed by cytarabine (Fig. 3B, right). In addition, these phenotypically defined LSC populations were not sensitive to doxorubicin (not shown). Consistently, functional assays confirmed the activity of AR-42 against leukemia stem and progenitor cells. Primary AML cells exposed to 0.25 μmol/L AR-42 had decreased colony-forming ability (Fig. 3C). Also, treatment of $CD34^+$ cord blood cells with AR-42 had minimal effect on myeloid and erythroid colony formation (Fig. 3D), suggesting that AR-42 does not inhibit normal hematopoietic progenitors. Furthermore, primary AML cells pretreated with 0.25 μmol/L AR-42 significantly decreased

engraftment into immunodeficient mice (Fig. 3E), demonstrating the ability of AR-42 to target LSCs, as does parthenolide (12).

To determine the effect of AR-42 in AML cells from an animal model, we used PU.1 hypomorphic (URE $^{\Delta/\Delta}$)mice for which LSC and pre-LSC populations have already been well characterized (36, 37). The animals develop an aggressive, transplantable AML with 100% penetrance [referred to as "*PU*.1 knockdown (KD) leukemia"; ref. 37). We tested the effect of AR-42 in URE $^{\Delta/\Delta}$ leukemia cells and found that growth and colony-forming ability of URE $^{\Delta/\Delta}$ leukemia cells was markedly inhibited by AR-42, whereas there were no significant effect observed with cytarabine (Fig. 3F and G). Importantly, treatment with AR-42 resulted in a complete loss of the replating ability of URE$^{\Delta/\Delta}$ leukemia cells (Fig. 3H). These results demonstrate that AR-42 has potent antileukemic activity in PU.1 hypomorphic (UREΔ/Δ) mouse leukemia cells. Taken together, we have demonstrated that as predicted by the *in silico* screen, AR-42 is a parthenolide-like compound that can ablate blast, stem, and progenitor cells (9, 12).

AR-42 inhibits NF-κB

Analysis of the AR-42 gene expression signature suggested the likelihood of AR-42–mediated NF-κB inhibition (Supplementary Table S1 and S3). Thus, we evaluated the effect of AR-42 on NF-κB activity using an ELISA-based binding assay and gene expression assays for NF-κB transcriptional targets. Indeed, AR-42 inhibited NF-κB–binding activity at concentrations <1 μmol/L using cell lines (Fig. 4A) and downregulated the expression of known NF-κB target genes such as *NFKB1*, *BCL2*, *MYB*, *PLAU*, *CDK6*, and *TNFSF13B* (refs. 38–43; Fig. 4B). This activity was also observed, as expected, for parthenolide-treated cells. These data support that AR-42, like parthenolide (9, 12), is, able to inhibit NF-κB pathways as predicted by the *in silico* screen.

AR-42 does not induce ROS or activate Nrf2 cytoprotective responses

We have previously reported that parthenolide and parthenolide-like compounds induce ROS, resulting in the activation of the transcription factor nuclear factor (erythroid-derived 2)-like 2(NFE2L2), also known as Nrf2 (9, 12, 13, 15). Nrf2 modulates the expression of genes involved in the regulation of oxidative stress. Thus, we evaluated the ability of AR-42 to induce oxidative stress and deplete thiols using flow cytometry assays with the fluorogenic probe CellROX and mBBr, respectively. We found that unlike parthenolide, AR-42 does not induce the production of ROS (Fig. 4C). In addition, the thiol depletion assay also shows that AR-42 exposure, unlike parthenolide, does not deplete thiols (Supplementary Fig. S3). Consistent with these data, the antileukemic activity of AR-42 could not be prevented by pretreatment with the anti-oxidant *N*-acetylcysteine (NAC), which has been shown for parthenolide (refs. 9, 12; Fig. 4D and Supplementary Fig. S3). In addition, we evaluated Nrf2 activation after treatment with AR-42 or parthenolide, using DNA-binding assays and qPCR for Nrf2 target genes, such as *HMOX1*, *NQO1* [NAD(P)H dehydrogenase (quinone) 1], and *GCLM* (glutamate-cysteine ligase regulatory subunit; ref. 15). As shown in Fig. 4E and F, AR-42 does not activate Nrf2, or Nrf2 target genes, consistent with the absence of ROS production. Consistently, we found that AR-42 did not induce heme oxygenase 1 protein expression as reported for parthenolide (Fig. 4G and

Supplementary Fig. S4). The absence of the activation of Nrf2 target genes was corroborated in FACS-purified stem/progenitor populations from primary AML samples, showing that AR-42 treatment does not result in the transcriptional activation of *HMOX1* (Fig. 4H). Taken together, these data demonstrate that AR-42, unlike parthenolide, does not induce ROS.

AR-42 activates caspase cascades

To determine the events involved in AR-42 induction of cell death in AML cells, we performed immunoblots to assess the induction of caspase cascades. We found cleaved PARP and cleaved caspase-8 at 6 hours of AR-42 treatment (1 μmol/L) concomitant with the decrease in phospho-p65 (Fig. 5A). Furthermore, we also found activation of caspase-3 by flow cytometry upon treatment with AR-42 (Fig. 5B). Together, these data demonstrate that AR-42 triggers caspase activation cascades in AML cells. Taken together, our data demonstrate that AR-42 treatment results in the activation of proapoptotic responses driven by caspase cleavage.

AR-42 displays a HSP90 inhibitory activity

AR-42 has been shown to inhibit the interaction of Hsp90 with client proteins in canine mast cells (44). Consistent with this report, we observed that HSPA1A encoding for one of Hsp70 isoforms was upregulated by both AR-42 and parthenolide (Fig. 1B). This transcriptional induction of Hsp70 has been reported as a consequence of HSP90 inhibition (45). Thus, we performed qPCR in purified stem and progenitor populations for HSPA1A after 6 hours of treatment with AR-42 or parthenolide. We corroborated the upregulation of HSP70 gene expression in all AML subpopulations (Fig. 5C). Furthermore, we evaluated whether AR-42 treatment disrupted the stability of known HSP90 client proteins such as FLT-3, AKT signaling pathway, and c-Kit (46–48). We found that AR-42 treatment resulted in the degradation of FLT-3 and pp70S6K, unlike parthenolide (Fig. 5D). In addition, AR-42, like the HSP90i PU-H71, resulted in HSP70 upregulation (Fig. 5E) and the degradation of FLT-3 and c-Kit (Fig. 5F and G), thus suggesting that AR-42 can inhibit HSP90 in AML cells as observed in canine mast cells (44). Importantly, c-Kit itself was also found to be downregulated at the transcriptional level by AR-42 and parthenolide (Fig. 1B). This observation is also consistent with a previous report that AR-42 can disrupt aberrant c-Kit expression (49).

Discussion

The goal of ablating cancer stem cells to prevent disease recurrence remains a significant therapeutic obstacle in numerous malignancies, including AML. We have previously shown that parthenolide, or its water-soluble analogue DMAPT, efficiently ablates AML at the bulk, stem, and progenitor level (9). Furthermore, we have shown that *in silico* approaches can be exploited to accelerate the identification of anti-LSC drugs with features similar to parthenolide (13). Specifically, using *in silico* screens, we identified two agents (celastrol and 4-hydroxy-nonenal; 4-HNE) as parthenolide-like agents. Both compounds, like parthenolide, were capable of inhibiting NF-κB and activating Nrf2 by upregulating ROS (12). Despite their efficacy, we more recently noted that the activation of Nrf2-regulated

detoxifying enzymes could elicit a cytoprotective response in AML cells (15). We later showed that by abrogating such responses the LSC sensitivity of AML cells to parthenolide can be increased (15, 16). In this report, transcriptional profiling of drug-induced gene perturbations identified that AR-42 exerts many similar effects to parthenolide (Fig. 1), but fails to induce ROS and transcriptional activation of Nrf2.

We first evaluated the sensitivity of different AML cell lines and primary AML samples to AR-42. The sensitivity of cells to parthenolide and cytarabine were also evaluated (Supplementary Fig. S2A and Fig. 2). Overall, most AML cell lines and primary AML samples were sensitive to AR-42 treatment, displaying LD_{50} in the submicromolar range (Table 2). AR-42 was able to induce cell death in most primary AML samples tested independent of their genetic aberrations, whereas parthenolide appeared to be less effective in TET2-mutant AML samples. We show that AR-42, in addition to killing AML blasts, can decrease viability of phenotypically defined LSCs ($CD34^+CD38^-CD123^+$; ref. 50) at submicromolar concentrations in contrast to cytarabine, which fails to eliminate LSCs (Fig. 3A and B). Importantly, we demonstrated the ability of AR-42 to target progenitor and stem cell population using xenotransplants and colony-forming assays. We found that treatment with AR-42 decreased AML colony formation and AML engraftment in immunodeficient mice (Fig. 3C and E). AR-42 had a minimal effect in normal myeloid colony formation (Fig. 3D), suggesting lower toxicity against normal hematopoietic progenitors. AR-42 was also effective in decreasing the colony formation of $URE^{\Delta/\Delta}$ AML cells, unlike cytarabine (Fig. 3F, G and H).

Since AR-42 was identified by the *in silico* screen as a parthenolide-like compound, we examined the molecular effects of AR-42 in AML cells shared with parthenolide. Parthenolide is a potent inhibitor of NF-κB (known to be constitutively activated in AML) (9, 10, 12). We demonstrated that AR-42, like parthenolide, is capable of inhibiting NF-κB using DNA-binding assays and gene expression assays for known NF-κB target genes (Fig. 4A and B). Parthenolide is also known to activate ROS and Nrf2-regulated detoxifying enzymes (15). We demonstrated that, unlike parthenolide, AR-42 does not induce ROS and its antileukemic activity is not blocked by NAC (Fig. 4C and D). Furthermore, AR-42 treatment does not increase Nrf2-binding activity or activate its transcriptional targets (Fig. 4E to 4H). Thus, among the commonalities of parthenolide and AR-42 is the ability to inhibit certain NF-κB target genes that are known to be important survival effectors such as *BCL2*, a novel activity for this HDAC inhibitor. However, AR-42 retains HDAC inhibitory activity producing varied transcriptional effects as revealed by both GSEA and immunoprecipitation assays (Supplementary Fig. S1). As such, a range of other gene expression alterations occur with AR-42 treatment.

To elucidate the cell death mechanisms evoked by AR-42, we evaluated the activation of caspases. We demonstrated that AR-42 induced cleavage of caspase-3, caspase-8, and PARP (Fig.5A and B). Furthermore, AR-42 has been described to block HSP90 interaction with its client proteins in canine mast cells (44). Consistently, we have also observed that its gene expression signature is also consistent with a HSP90 inhibitory activity (increased expression of HSP70; Fig. 1B; ref. 45). We found that AR-42 upregulated HSP70 and

resulted in the degradation of known AML client proteins (Fig. 5C–G). Taken together, we found that AR-42 can also inhibit HSP90 in AML as observed in canine mast cells (44).

In summary, we identified AR-42 as a novel agent that can ablate AML cells at the bulk, stem, and progenitor cell level using *in silico* approaches. Our studies revealed an undescribed NF-κB inhibitory activity for AR-42. Furthermore, AR-42 did not induce ROS or activated Nrf2 transcriptional targets such as heme oxygenase I. Finally, we confirmed that in AML cells AR-42 displays an Hsp90 inhibitory activity as observed in canine mast cells (44). AR-42 is currently in clinical trial for patients with AML in combination with decitabine (clinical trials.gov, NCT0179891).

Supplementary Material

Refer to Web version on PubMed Central for supplementary material.

Acknowledgments

The authors thank Dr. Ulrich Steidl for kindly providing the URE$^{\Delta/\Delta}$ leukemia cells and Dr. Hongliang Zong and Jeanne De Leon for their input in the article.

Grant Support: This work was partially funded by ARNO Therapeutics. M.L. Guzman is funded by the NIH through the NIH Director's New Innovator Award Program, 1 DP2 OD007399-01, NCI (R21 CA158728-01A1), Leukemia and Lymphoma Foundation (LLS 6330-11 and LLS 6427-13). M.L. Guzman is a V Foundation Scholar. D.C. Hassane is funded through the LLS (LLS 6453-13) and G. Marcucci and M.L. Guzman are funded by R01CA158350.

References

1. Lapidot T, Sirard C, Vormoor J, Murdoch B, Hoang T, Caceres-Cortes J, et al. A cell initiating human acute myeloid leukaemia after transplantation into SCID mice. Nature. 1994; 367:645–8. [PubMed: 7509044]
2. Bonnet D, Dick JE. Human acute myeloid leukemia is organized as a hierarchy that originates from a primitive hematopoietic cell. Nat Med. 1997; 3:730–7. [PubMed: 9212098]
3. van Rhenen A, Feller N, Kelder A, Westra AH, Rombouts E, Zweegman S, et al. High stem cell frequency in acute myeloid leukemia at diagnosis predicts high minimal residual disease and poor survival. Clin Cancer Res. 2005; 11:6520–7. [PubMed: 16166428]
4. van Stijn A, Feller N, Kok A, van der Pol MA, Ossenkoppele GJ, Schuurhuis GJ. Minimal residual disease in acute myeloid leukemia is predicted by an apoptosis-resistant protein profile at diagnosis. Clin Cancer Res. 2005; 11:2540–6. [PubMed: 15814631]
5. Gerber JM, Smith BD, Ngwang B, Zhang H, Vala MS, Morsberger L, et al. A clinically relevant population of leukemic CD34(þ)CD38(-) cells in acute myeloid leukemia. Blood. 2012; 119:3571–7. [PubMed: 22262762]
6. Eppert K, Takenaka K, Lechman ER, Waldron L, Nilsson B, van Galen P, et al. Stem cell gene expression programs influence clinical outcome in human leukemia. Nat Med. 2011; 17:1086–93. [PubMed: 21873988]
7. Gentles AJ, Plevritis SK, Majeti R, Alizadeh AA. Association of a leukemic stem cell gene expression signature with clinical outcomes in acute myeloid leukemia. JAMA. 2010; 304:2706–15. [PubMed: 21177505]
8. Guan Y, Gerhard B, Hogge DE. Detection, isolation, and stimulation of quiescent primitive leukemic progenitor cells from patients with acute myeloid leukemia (AML). Blood. 2003; 101:3142–9. [PubMed: 12468427]

9. Guzman ML, Rossi RM, Neelakantan S, Li X, Corbett CA, Hassane DC, et al. An orally bioavailable parthenolide analog selectively eradicates acute myelogenous leukemia stem and progenitor cells. Blood. 2007; 110:4427–35. [PubMed: 17804695]
10. Guzman ML, Neering SJ, Upchurch D, Grimes B, Howard DS, Rizzieri DA, et al. Nuclear factor-kappaB is constitutively activated in primitive human acute myelogenous leukemia cells. Blood. 2001; 98:2301–7. [PubMed: 11588023]
11. Guzman ML, Swiderski CF, Howard DS, Grimes BA, Rossi RM, Szilvassy SJ, et al. Preferential induction of apoptosis for primary human leukemic stem cells. Proc Natl Acad Sci U S A. 2002; 99:16220–5. [PubMed: 12451177]
12. Guzman ML, Rossi RM, Karnischky L, Li X, Peterson DR, Howard DS, et al. The sesquiterpene lactone parthenolide induces apoptosis of human acute myelogenous leukemia stem and progenitor cells. Blood. 2005; 105:4163–9. [PubMed: 15687234]
13. Hassane DC, Guzman ML, Corbett C, Li X, Abboud R, Young F, et al. Discovery of agents that eradicate leukemia stem cells using an *in silico* screen of public gene expression data. Blood. 2008; 111:5654–62. [PubMed: 18305216]
14. Sweeney CJ, Mehrotra S, Sadaria MR, Kumar S, Shortle NH, Roman Y, et al. The sesquiterpene lactone parthenolide in combination with docetaxel reduces metastasis and improves survival in a xenograft model of breast cancer. Mol Cancer Ther. 2005; 4:1004–12. [PubMed: 15956258]
15. Hassane DC, Sen S, Minhajuddin M, Rossi RM, Corbett CA, Balys M, et al. Chemical genomic screening reveals synergism between parthenolide and inhibitors of the PI-3 kinase and mTOR pathways. Blood. 2010; 116:5983–90. [PubMed: 20889920]
16. Sen S, Hassane DC, Corbett C, Becker MW, Jordan CT, Guzman ML. Novel mTOR inhibitory activity of ciclopirox enhances parthenolide antileukemia activity. Exp Hematol. 2013; 41:799–807 e4. [PubMed: 23660068]
17. Kulp SK, Chen CS, Wang DS, Chen CY, Chen CS. Antitumor effects of a novel phenylbutyrate-based histone deacetylase inhibitor, (S)-HDAC-42, in prostate cancer. Clin Cancer Res. 2006; 12:5199–206. [PubMed: 16951239]
18. Lu Q, Yang YT, Chen CS, Davis M, Byrd JC, Etherton MR, et al. Zn2+-chelating motif-tethered short-chain fatty acids as a novel class of histone deacetylase inhibitors. J Med Chem. 2004; 47:467–74. [PubMed: 14711316]
19. Zhang S, Suvannasankha A, Crean CD, White VL, Chen CS, Farag SS. The novel histone deacetylase inhibitor, AR-42, inhibits gp130/Stat3 pathway and induces apoptosis and cell cycle arrest in multiple myeloma cells. Int J Cancer. 2011; 129:204–13. [PubMed: 20824695]
20. Lucas DM, Alinari L, West DA, Davis ME, Edwards RB, Johnson AJ, et al. The novel deacetylase inhibitor AR-42 demonstrates pre-clinical activity in B-cell malignancies *in vitro* and *in vivo*. PLoS ONE. 2010; 5:e10941. [PubMed: 20532179]
21. Johnstone RW. Histone-deacetylase inhibitors: novel drugs for the treatment of cancer. Nat Rev Drug Discov. 2002; 1:287–99. [PubMed: 12120280]
22. Lansdorp PM, Dragowska W. Long-term erythropoiesis from constant numbers of CD34þ cells in serum-free cultures initiated with highly purified progenitor cells from human bone marrow. J Exp Med. 1992; 175:1501–9. [PubMed: 1375263]
23. Gentleman RC, Carey VJ, Bates DM, Bolstad B, Dettling M, Dudoit S, et al. Bioconductor: open software development for computational biology and bioinformatics. Genome Biol. 2004; 5:R80. [PubMed: 15461798]
24. Dunning MJ, Smith ML, Ritchie ME, Tavare S. beadarray: R classes and methods for Illumina bead-based data. Bioinformatics. 2007; 23:2183–4. [PubMed: 17586828]
25. Subramanian A, Tamayo P, Mootha VK, Mukherjee S, Ebert BL, Gillette MA, et al. Gene set enrichment analysis: a knowledge-based approach for interpreting genome-wide expression profiles. Proc Natl Acad Sci U S A. 2005; 102:15545–50. [PubMed: 16199517]
26. Smyth, G. Limma: linear models for microarray data. New York, NY: Springer; 2005.
27. Benjamini Y, H Y. Controlling the false discovery rate: a practical and powerful approach to multiple testing. J R Statist Soc B. 1995; 57:289–300.

28. Dennis G Jr, Sherman BT, Hosack DA, Yang J, Gao W, Lane HC, et al. DAVID: database for annotation, visualization, and integrated discovery. Genome Biol. 2003; 4:P3. [PubMed: 12734009]
29. Yu, G. R package version 1.2.1 ReactomePA: Bioconductor. Reactome pathway analysis.
30. Yu G, Wang LG, Han Y, He QY. clusterProfiler: an R package for comparing biological themes among gene clusters. OMICS. 2012; 16:284–7. [PubMed: 22455463]
31. Csardi G, N T. The igraph software package for complex network research. InterJournal, Complex Systems. 2006; 1695
32. Shannon P, Markiel A, Ozier O, Baliga NS, Wang JT, Ramage D, et al. Cytoscape: a software environment for integrated models of biomolecular interaction networks. Genome Res. 2003; 13:2498–504. [PubMed: 14597658]
33. Beyer, S.; Kulp, S.; Baird, M.; Auer, H.; Kornacker, K.; Chen, CS., et al. The effects of a phenylbutyrate-derived histone deacetylase inhibitor (HDAC-42) on acid-induced gene expression patterns of SEG-1 human esophageal adenocarcinoma cells. Proceedings of the Annual Meeting of the American Association for Cancer Research; Washington, DC. Philadelphia (PA). AACR; 2006. p. 1128-9.abstract2006
34. Ley TJ, Ding L, Walter MJ, McLellan MD, Lamprecht T, Larson DE, et al. DNMT3A mutations in acute myeloid leukemia. N Engl J Med. 2010; 363:2424–33. [PubMed: 21067377]
35. Saito Y, Uchida N, Tanaka S, Suzuki N, Tomizawa-Murasawa M, Sone A, et al. Induction of cell cycle entry eliminates human leukemia stem cells in a mouse model of AML. Nat Biotechnol. 2010; 28:275–80. [PubMed: 20160717]
36. Steidl U, Rosenbauer F, Verhaak RG, Gu X, Ebralidze A, Otu HH, et al. Essential role of Jun family transcription factors in PU. 1 knockdowninduced leukemic stem cells. Nat Genet. 2006; 38:1269–77. [PubMed: 17041602]
37. Rosenbauer F, Owens BM, Yu L, Tumang JR, Steidl U, Kutok JL, et al. Lymphoid cell growth and transformation are suppressed by a key regulatory element of the gene encoding PU. 1. Nat Genet. 2006; 38:27–37. [PubMed: 16311598]
38. Toth CR, Hostutler RF, Baldwin AS Jr, Bender TP. Members of the nuclear factor kappa B family transactivate the murine c-myb gene. J Biol Chem. 1995; 270:7661–71. [PubMed: 7706314]
39. Ten RM, Paya CV, Israel N, Le Bail O, Mattei MG, Virelizier JL, et al. The characterization of the promoter of the gene encoding the p50 subunit of NF-kappa B indicates that it participates in its own regulation. EMBO J. 1992; 11:195–203. [PubMed: 1740105]
40. Novak U, Cocks BG, Hamilton JA. A labile repressor acts through the NFkB-like binding sites of the human urokinase gene. Nucleic Acids Res. 1991; 19:3389–93. [PubMed: 1905804]
41. Moon EY, Park H. B cell activating factor (BAFF) gene promoter activity depends upon co-activator, p300. Immunobiology. 2007; 212:637–45. [PubMed: 17869641]
42. Iwanaga R, Ozono E, Fujisawa J, Ikeda MA, Okamura N, Huang Y, et al. Activation of the cyclin D2 and cdk6 genes through NF-kappaB is critical for cell-cycle progression induced by HTLV-I Tax. Oncogene. 2008; 27:5635–42. [PubMed: 18504428]
43. Catz SD, Johnson JL. Transcriptional regulation of bcl-2 by nuclear factor kappa B and its significance in prostate cancer. Oncogene. 2001; 20:7342–51. [PubMed: 11704864]
44. Lin TY, Fenger J, Murahari S, Bear MD, Kulp SK, Wang D, et al. AR-42, a novel HDAC inhibitor, exhibits biologic activity against malignant mast cell lines via down-regulation of constitutively activated Kit. Blood. 2010; 115:4217–25. [PubMed: 20233974]
45. Neckers L, Workman P. Hsp90 molecular chaperone inhibitors: are we there yet? Clin Cancer Res. 2012; 18:64–76. [PubMed: 22215907]
46. Stravopodis DJ, Margaritis LH, Voutsinas GE. Drug-mediated targeted disruption of multiple protein activities through functional inhibition of the Hsp90 chaperone complex. Curr Med Chem. 2007; 14:3122–38. [PubMed: 18220746]
47. Wang Y, Trepel JB, Neckers LM, Giaccone G. STA-9090, a smallmolecule Hsp90 inhibitor for the potential treatment of cancer. Curr Opin Investig Drugs. 2010; 11:1466–76.
48. Basso AD, Solit DB, Chiosis G, Giri B, Tsichlis P, Rosen N. Akt forms an intracellular complex with heat shock protein 90 (Hsp90) and Cdc37 and is destabilized by inhibitors of Hsp90 function. J Biol Chem. 2002; 277:39858–66. [PubMed: 12176997]

49. Liu S, Wu LC, Pang J, Santhanam R, Schwind S, Wu YZ, et al. Sp1/ NFkappaB/HDAC/miR-29b regulatory network in KIT-driven myeloid leukemia. Cancer Cell. 2010; 17:333–47. [PubMed: 20385359]

50. Jordan CT, Upchurch D, Szilvassy SJ, Guzman ML, Howard DS, Pettigrew AL, et al. The interleukin-3 receptor alpha chain is a unique marker for human acute myelogenous leukemia stem cells. Leukemia. 2000; 14:1777–84. [PubMed: 11021753]

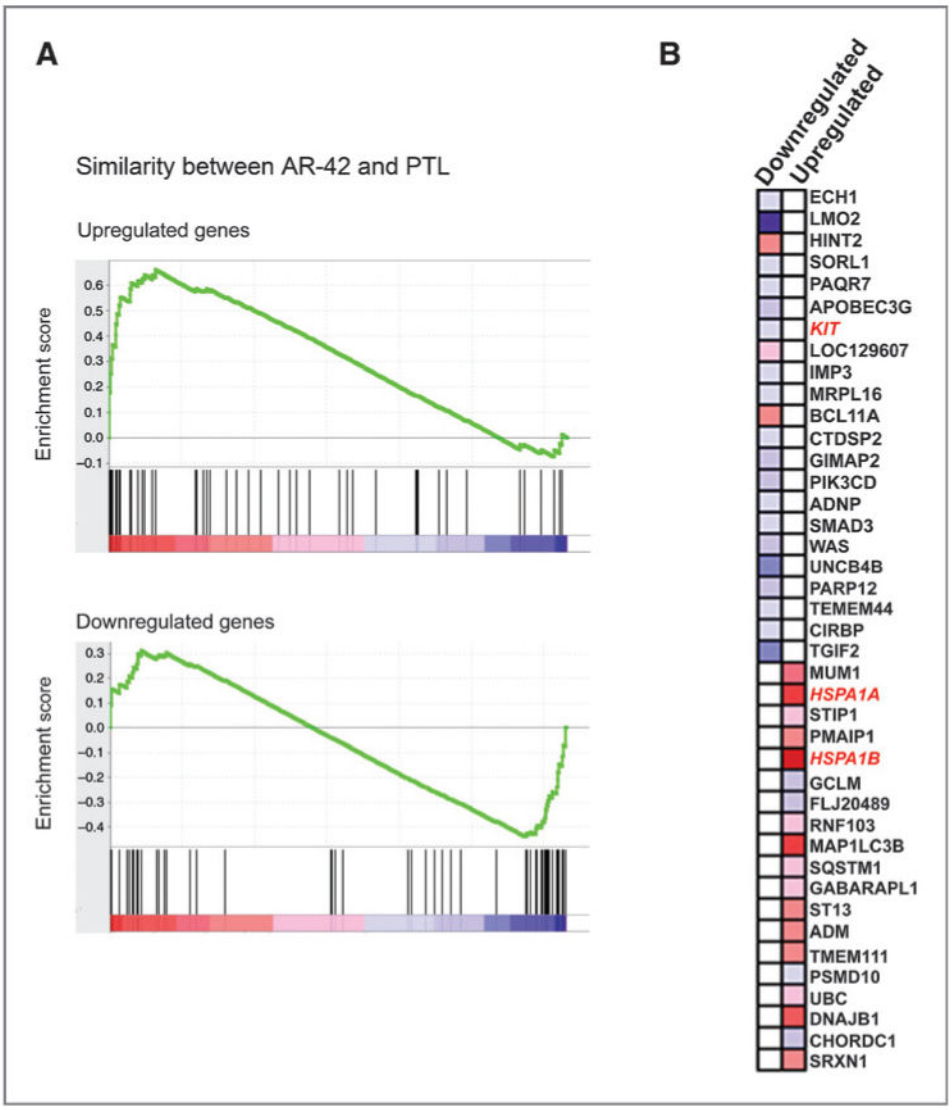

Figure 1.

AR-42 can evoke parthenolide-like transcriptional perturbations. A, GSEA indicates similarity between AR-42 and parthenolide for genes both upregulated (top) and downregulated (bottom) by parthenolide. Vertical lines represent instances of a gene reported to be upregulated (top) and downregulated (bottom) by parthenolide on a rank-ordered list of AR-42–induced fold changes. B, heatmap of parthenolide upregulated and downregulated leading-edge genes in the AR-42 gene signature. Downregulation of *KIT* and upregulation of *HSP70* occur.

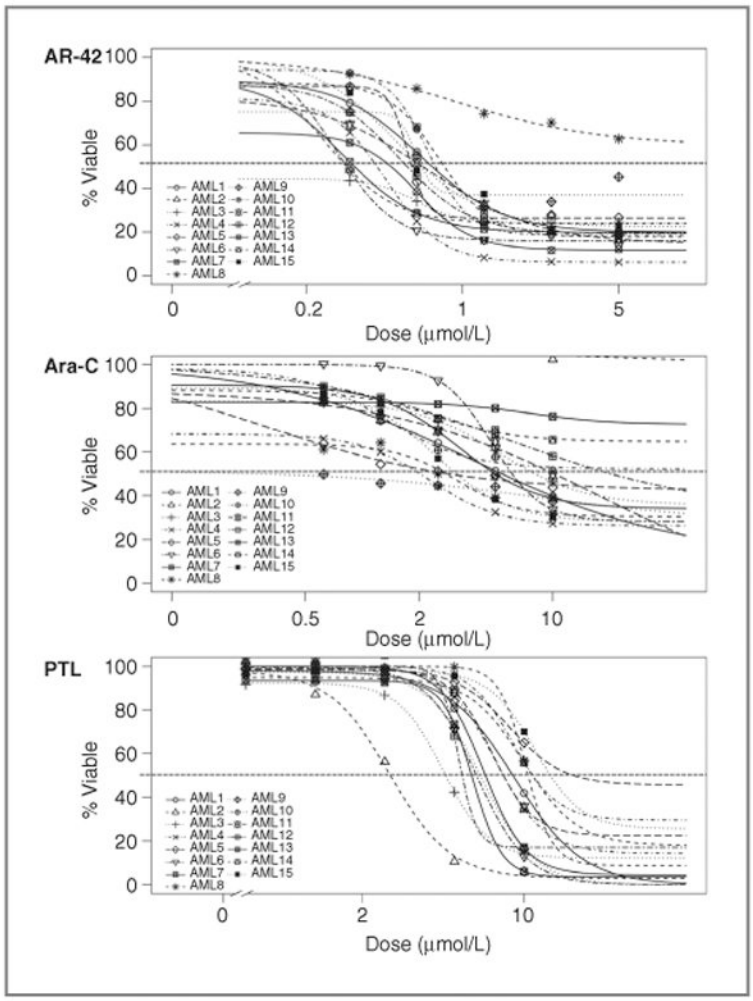

Figure 2.

AR-42 demonstrates activity against different primary AML samples bearing different genetic mutations in contrast to cytarabine (Ara-C) and parthenolide. Dose–response curves were generated after 48 hours of treatment with either AR-42 (top), cytarabine (Ara-C; middle), or parthenolide (parthenolide; bottom). Graphs are represented as percent viability relative to untreated control versus concentration (µmol/L). Each line represents a primary AML specimen. Viability was measured by flow cytometry using Annexin-V/7-AAD staining. FLT3-ITD–positive AML (AML1, 4, 8, 11, 12, 14, and 15); TET2-mutant AML (AML 5, 8, 9, and 13), DNMT3 mutant (AML 4, 11, 12, and 14).

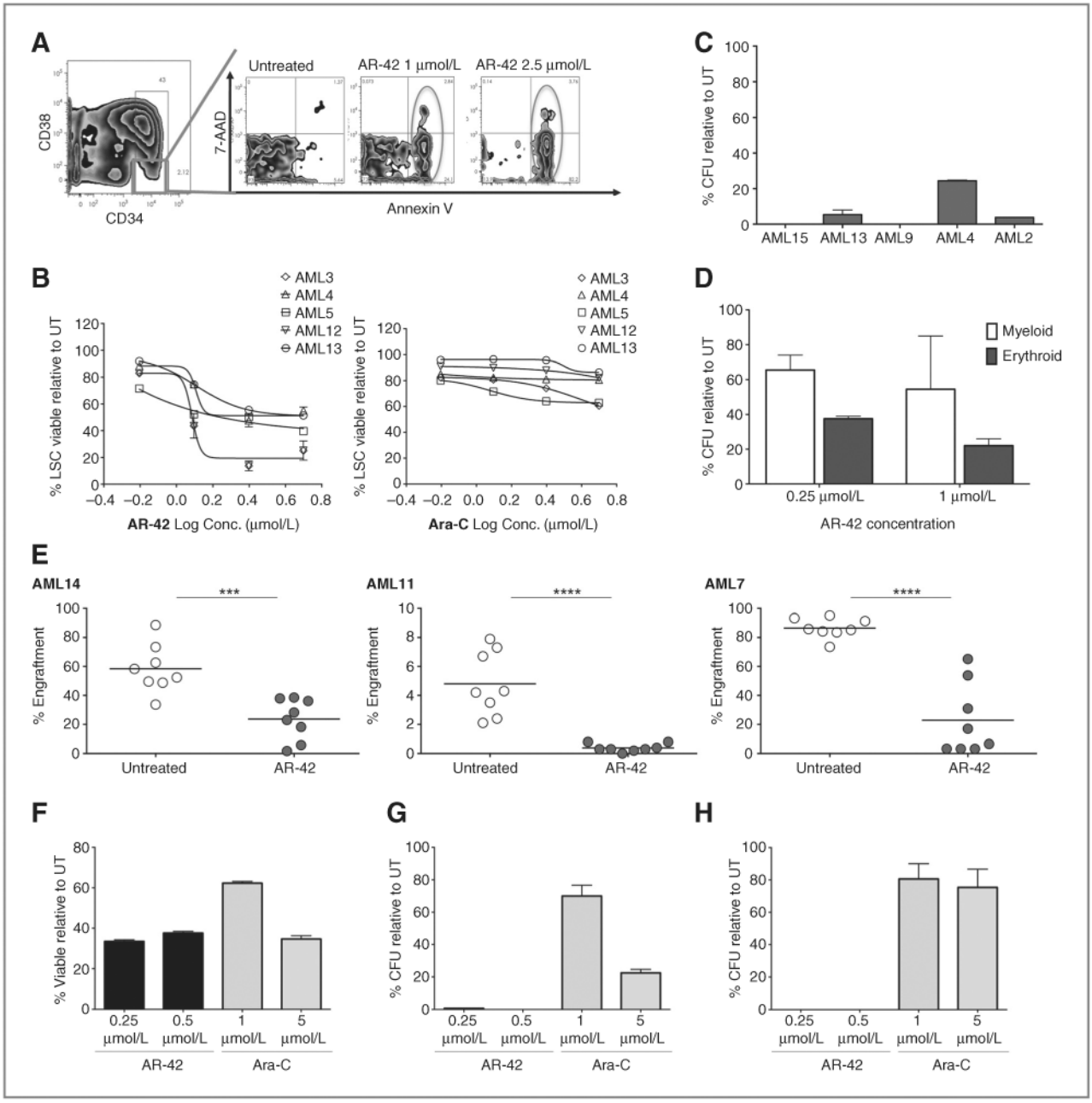

Figure 3.

AR-42 demonstrates activity against LSCs. A, gating strategy for flow cytometry analyses for primary AML cells. B, percent viability in LSC subpopulations from primary AML samples after 48 hours of treatment with either cytarabine (Ara-C) or AR-42. Graphs are represented as percent viability relative to untreated control versus log concentration (µmol/L). Each line represents a primary AMLspecimen. C, colony-forming units (CFU) of primary human AML cells treated with AR-42 (0.25 µmol/L) relative to control represented as a percentage. D, CFU for human $CD34^+$ cord blood (CB) cells treated with AR-42 at the indicated concentrations relative to control represented as percentage. Dark bars, erythroid

colonies; white bars, myeloid colonies. Error bars, SEM. E, percent of bone marrow engraftment for NOD/SCID mice transplanted with AML cells after 18 hours of culture with or without AR-42 treatment. Each circle represents a single animal analyzed at 6 weeks after transplantation. Mean engraftment is indicated by the horizontal bars. ***, $P < 0.001$; ****, $P < 0.0001$. F, AR-42 is highly effective at inhibiting growth UREΔ/Δ AML cells. Cell viability in suspension culture upon treatment with two different concentrations of AR-42 and cytarabine is equally effective at killing AML cells but at 10-fold lower concentrations of AR-42 in comparison with cytarabine. G, AR-42 has a very profound effect on the clonogenicity of UREΔ/Δ AML cells and completely suppresses their serial replating capacity *in vitro* (H).

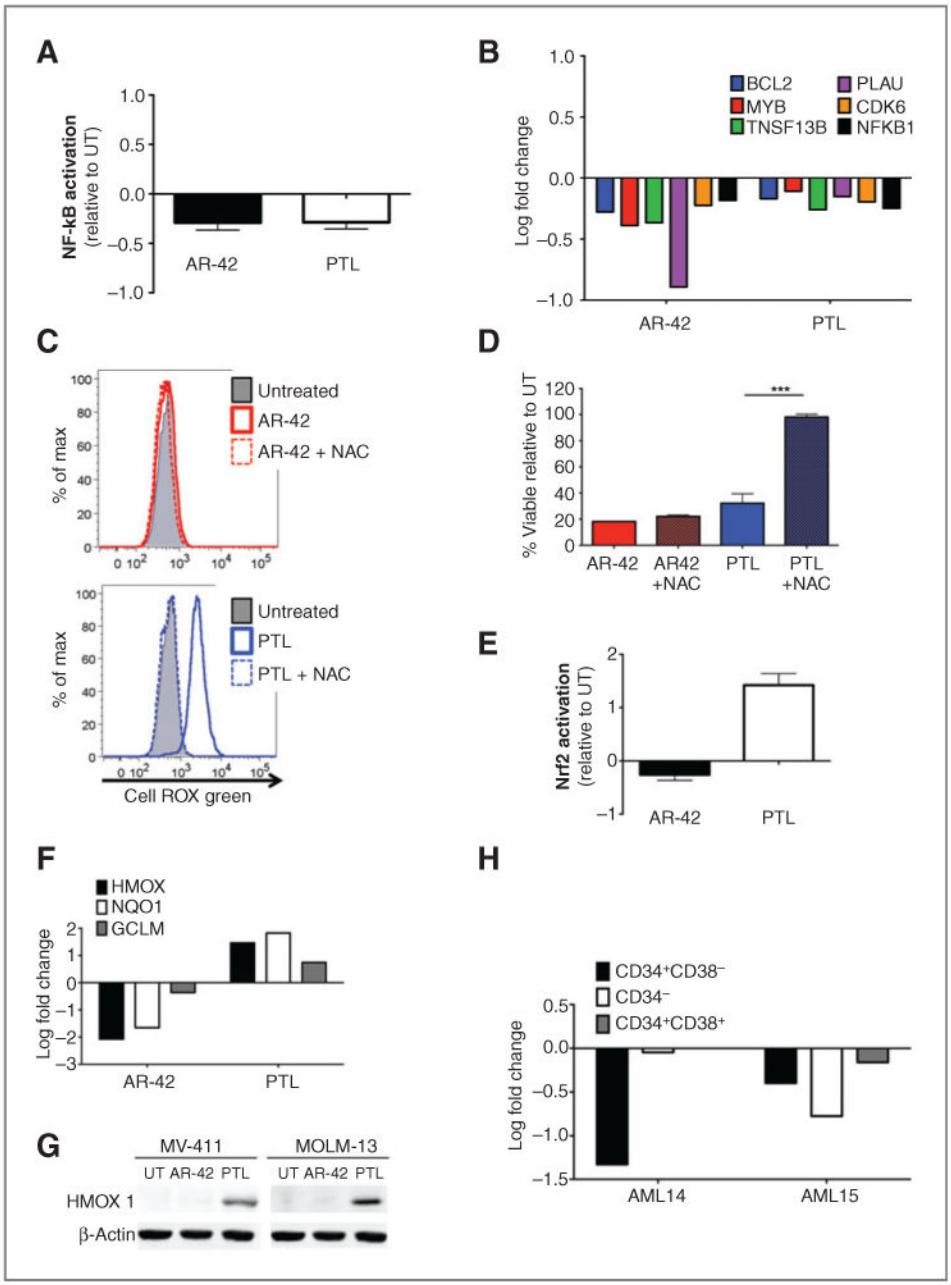

Figure 4.

AR-42 inhibits NF-κb and does not activate Nrf2. A, NF-κb binding activity evaluated by DNA binding ELISA 6 hours after treatment with either AR-42 or parthenolide. B, gene expression analysis for NF-κb target genes: *NFKB1*, *BCL2*, *MYB*, *TNSF13B*, *PLAU*, and *CDK6* in primary AML cells. Log10 fold change in expression shown. C, flow cytometry histograms for intracellular ROS using CellRox staining 6 hours after treatment with AR-42 or parthenolide, ± NAC. D, percent viability of MV4-11 cells after 48 hours of treatment with AR-42 or parthenolide (PTL) in the presence or absence of NAC. Graphs indicate the percent viability relative to untreated control. Viability was evaluated by flow cytometry using annexin V/7-AAD staining. ***, $P < 0.001$. E, Nrf2-binding activity evaluated using a

DNA-binding ELISA 6 hours after treatment with either AR-42 or parthenolide. F, gene expression analysis for Nrf2 target genes: *HMOX-1*, *NQO1*, and *GCLM* in primary AML cells. Log_{10} fold change in expression shown. G, mmunoblot for HMOX-1 or β-actin after 6 hours of treatment with either AR-42 or parthenolide. H, gene expression analysis for *HMOX-1* in purified primary AML populations after 6 hours of treatment with AR-42. Log_{10} fold change in expression shown.

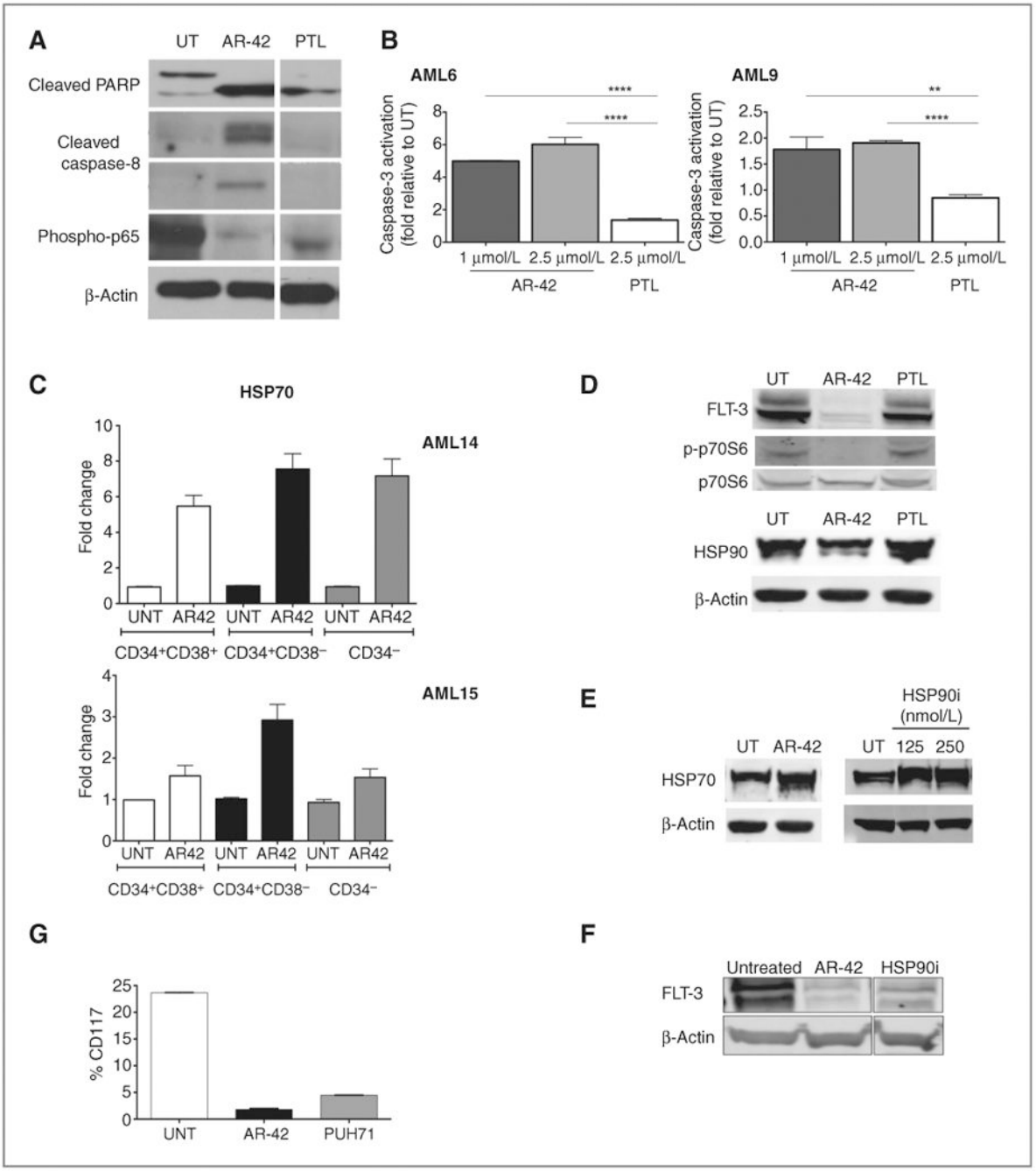

Figure 5.

AR-42 activates caspase cascades and inhibits HSP90. A, immunoblot for MV4-11 cells after 6 hours of treatment with AR-42 (1 μmol/L) or parthenolide (7.5 μmol/L). Blot was probed for cleaved PARP, cleaved caspase-8, phospho-p65, and β-actin antibodies. B, fold change in expression of active caspase-3 in primary AML cells after 6 hours of treatment with the indicated concentrations of AR-42 or parthenolide relative to control. Active caspase-3 was evaluated by flow cytometry. Error bars, SEM. **, $P < 0.01$; ****, $P < 0.0001$, significance evaluated by one-way ANOVA. C, gene expression analysis for

HSPA1A in purified primary AML populations after 6 hours of treatment with AR-42. Log fold change in expression shown. D, immunoblot for MV4-11 cells after treatment with (1 μmol/L) AR-42 or (7.5 μmol/L) parthenolide. Blot was probed for FLT-3, p-P70S6K, and HSP90 antibodies. Total p70S6K and β-actin are shown as the loading control. See Supplementary Fig. S5 for quantification. E, immunoblot analysis of HSP70 in MOLM-13 cells after 6 hours of treatment with (1 μmol/L) AR-42 or (0.25 μmol/L) PU-H71 (HSP90i). β-Actin is shown as the loading control. See Supplementary Fig. S5 for quantification. F, immunoblot for MV4-11 cells after 24 hours of treatment with AR-42 (1 μmol/L) or PU-H71 (HSP90i; 0.25 μmol/L). Blot was probed for FLT-3 and (β-actin antibodies. G, percentage of $CD117^+$ cells 6 hours after treatment with (1 μmol/L) AR-42 or (0.25 μmol/L) HSP90i.

Table 1
Clinical characteristics of the primary AML specimens tested

Sample	Sample information	FLT3-ITD	Other mutations
AML1	N/A	Positive	
AML2	M4; normal cytogenetics; relapsed	Positive	DNMT3A
AML3	N/A	Positive	
AML4	M2; normal cytogenetics; *de novo*	Positive	DNMT3A
AML5	MDS progression to AML	Positive	DNMT3A
AML6	N/A	Negative	
AML7	N/A	Negative	TET2
AML8	N/A	Negative	TET2
AML9	N/A	Negative	
AML10	inv16 (p13.1q22) (5)/47idem, +22[15]; relapsed AML	Positive	
AML11	Normal cytogenetics	Negative	TET2
AML12	N/A	Positive	DNMT3A
AML13	N/A	Negative	
AML14	N/A	Negative	
AML15	Refractory	Positive	

Abbreviation: N/A, not available.

Table 2

LD_{50} values for AR-42–treated AML cell lines and primary AML specimens

	Estimated LD_{50} (μmol/L)
AML cell lines	
HL-60	0.531
Kasumi-1	0.417
KG-1	0.453
MOLM13	0.594
MV4-11	0.344
TF-1	0.410
THP-1	NA
TUR	0.945
U937	0.606
Primary AML samples	
AML1	0.731
AML2	0.303
AML3	<0.25[a]
AML4	0.415
AML5	0.594
AML6	0.303
AML7	0.328
AML8	>5[a]
AML9	0.656
AML10	0.758
AML11	0.664
AML12	0.566
AML13	0.479
AML14	0.829
AML15	0.660

[a]Not computable within the concentrations evaluated.